European Polymer Journal 49 (2013) 3770–3777

Contents lists available at ScienceDirect

European Polymer Journal

journal homepage: www.elsevier.com/locate/europolj

Macromolecular Nanotechnology

Polymerized ionic liquid functionalized multi-walled carbon nanotubes/polyetherimide composites

Meltem Tunckol [a], Ester Zuza Hernandez [b], Jose-Ramon Sarasua [b], Jérôme Durand [a], Philippe Serp [a,*]

[a] Laboratoire de Chimie de Coordination, UPR CNRS 8241, Composante ENSIACET, Université de Toulouse UPS-INP-LCC, 4 allée Emile Monso, CS 44362, 31030 Toulouse Cedex 4, France

[b] Department of Mining-Metallurgy Engineering and Materials Science, Basque Excellence Research Center for Macromolecular Design and Engineering POLYMAT, School of Engineering, University of the Basque Country (UPV/EHU), Alameda de Urquijo s/n, 48013 Bilbao, Spain

ARTICLE INFO

Article history:
Received 19 February 2013
Received in revised form 16 July 2013
Accepted 4 August 2013
Available online 19 August 2013

Keywords:
Carbon nanotubes
Polymer–matrix composites
Ionic liquids
polyetherimide

ABSTRACT

Thin polyetherimide (PEI) films containing 0.1–3 wt.% multi-walled carbon nanotubes (MWCNTs), have been prepared from three types of MWCNTs, namely pristine, oxidized and polymerized ionic liquid (PIL) functionalized CNTs. Oxidized and PIL functionalized CNTs (CNT–PIL) showed better dispersion in the matrix compared to pristine CNTs. For CNT–PIL, alignment of CNTs has been observed in the matrix. Regardless of the type of CNTs, their incorporation led to an increased thermal stability of the polymer matrix. Dynamic mechanical analysis showed that storage modulus increased by up to 25% (3 wt.% CNT–PIL) and an increase in the height of the damping peaks ($\tan\delta$). The addition of CNTs did not have any significant influence on the tensile properties and T_g of the polymer, and the electrical conductivity did not decrease in the case of modified CNTs.

1. Introduction

Carbon nanotubes (CNTs) are ideal candidates as reinforcing and electrically conducting fillers for high strength and light-weight multifunctional polymer composites. However, there are several challenges for developing such composites, including homogeneous dispersion of CNTs in the polymeric matrix and strong interfacial adhesion [1]. In that context, many efforts have been devoted during the last two decades to surface modification of CNTs using covalent or non-covalent approaches [2]. The non-covalent route is particularly attractive due to its ease of operation and to the fact that it does not alter CNT structure. Ionic liquids (ILs) can provide an easy way to prepare CNT–IL hybrids, owing to cation-π, π–π or van der Waals interactions [3]. These hybrids can be further processed to prepare polymer composites using solution- or melt-processing methods. Due to their high-thermal stability, these hybrids can withstand the high temperatures used during the processing of polymers, and their solubility can be tuned by selecting the appropriate IL counter anion. Polymerized ionic liquids (PILs), have recently attracted attention as a new class of CNT modifiers. The thin PIL layer on the CNT surface can provide stable binding sites for polymer matrices to attach. The number of studies devoted to polymer composites filled with PIL-functionalized CNTs is still very limited [4]. Polyetherimide (PEI) is a high-performance thermoplastic, which has extensive uses in many fields such as medicine, electronics, automotive and aerospace. The extremely high viscosity of this polymer makes the nanocomposite preparation by melt-processing challenging [5]. Solution-based processing methods offer advantages of lower viscosities, which facilitate dispersion, provided highly stable dispersions of CNTs are used. Different surface modification approaches, including acid-oxidation and use of surfactants, have been applied to CNTs in order to obtain stable dispersions in suitable solvents for

* Corresponding author. Tel.: +33 5 34 32 35 72; fax: +33 5 34 32 35 96.
E-mail address: philippe.serp@ensiacet.fr (P. Serp).

0014-3057/$ - see front matter © 2013 Elsevier Ltd. All rights reserved.
http://dx.doi.org/10.1016/j.eurpolymj.2013.08.007

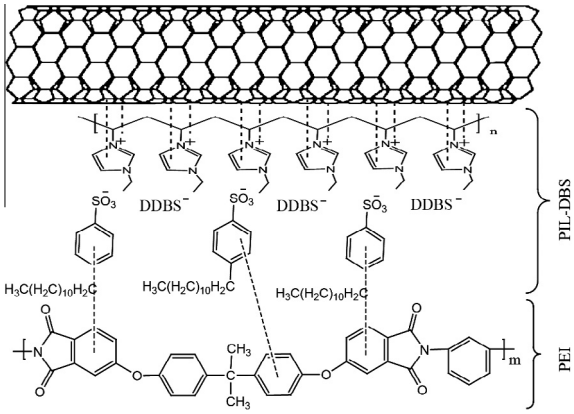

Fig. 1. Illustration of the possible non-covalent interaction between poly([VEIM]DBS) functionalized CNTs and PEI.

PEI processing [6–8]. In these studies, thermal stabilities of the composites improved significantly while improvements in mechanical properties are not remarkable; and in some cases [7,8] negative effects of CNT addition have been observed on the tensile strength. We anticipated that coating a thin film of PIL on CNT surface could result in a better adhesion between CNT and the PEI matrix. The PIL layer could act as a linker between the CNT and the matrix by possible π–π stacking interactions (Fig. 1). We report herein the introduction of multi-walled CNTs (MWCNTs) non-covalently functionalized with poly(1-vinyl-3-ethyl imidazolium) dodecylbenzene sulfonate (poly[VEIM]DBS) into PEI matrix and its effect on the morphological, mechanical, thermal and electrical properties of the composites.

2. Experimental details

2.1. Materials

Polyetherimide in pellet form was supplied by SABIC Innovative Plastics TM. Graphistrength® MWCNTs (average number of walls 5–15, length 0.1–10 μm, diameter 10–15 nm, purity >90%) were supplied by Arkema, France. Sodium dodecylbenzene sulfonate was purchased from Aldrich. Oxidized CNTs were prepared from pristine CNTs by: (i) purification in boiling concentrated H_2SO_4 followed by filtration and washing with water and (ii) refluxing purified CNTs in concentrated nitric acid (69%) for 3 h [9,10]. The surface acidic group concentration on oxidized CNTs was estimated to be 0.234 mmol/g CNT by acid–base titration [11]. Synthesis and polymerization of 1-vinyl-3-ethyl-imidazolium bromide ([VEIM]Br) were carried out as reported in literature [12]. Poly(1-vinyl-3-ethyl-imidazolium dodecylbenzene sulfonate) (poly[VEIM]DBS) was prepared using an anion exchange method previously reported [13]. Their structures were confirmed by ^{1}H NMR analysis (Fig. S1 in Supplementary Data (SD)). The glass transition temperatures (T_g) of poly[VEIM]Br and poly[VEIM]DBS were found to be 229 °C and 114 °C, respectively, as determined by DSC (20 °C min^{-1}).

2.2. Preparation of PIL functionalized CNTs

The non-covalent functionalization of CNTs was carried out using the following procedure: pristine CNTs (4 g) were added to a solution of [VEIM]Br (73 g) in ethanol (100 mL). After sonication with an ultrasonic bath cleaner for 1 h, azobis(isobutyronitrile) (AIBN, 1.5 g) was added to the mixture, which was stirred vigorously at 65 °C for 24 h under a N_2 atmosphere. The resulted CNTs were washed several times with distilled water in order to thoroughly remove physically adsorbed polymer and unreacted monomer from their surface. To prepare CNT–poly[VEIM]DBS, 500 mg of CNT–poly[VEIM]Br were added to 75 mL of distilled water, and the solution was ultrasonicated at 25% amplitude for 10 min. Then, a solution of sodium dodecylbenzene sulfonate (500 mg) in distilled water (25 mL) was added dropwise to the CNT suspension. The dispersion was stirred overnight and the resulted CNTs were thoroughly washed with distilled water and dried at 115 °C for 3 days.

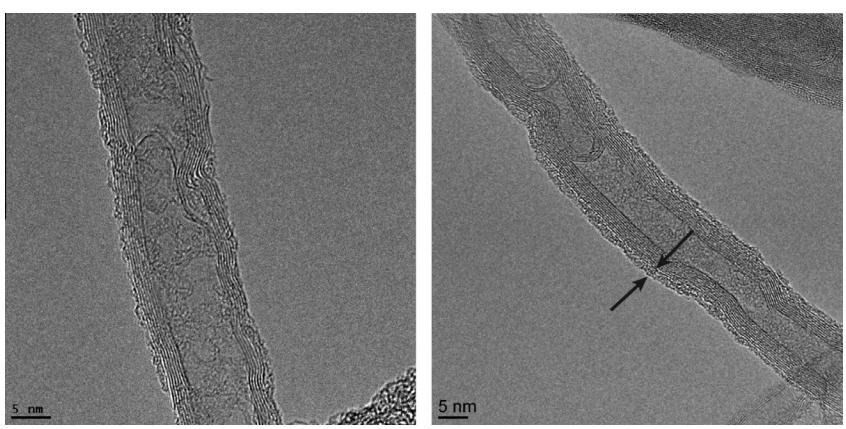

Fig. 2. TEM micrograph of pristine CNT used in this study (left) and CNT–poly[VEIM]DBS (right).

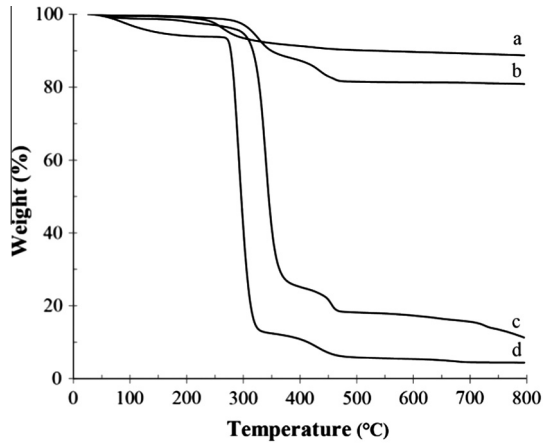

Fig. 3. TGA profiles of (a) CNT–poly[VEIM]Br, (b) CNT–poly[VEIM]DBS, (c) poly[VEIM]DBS and (d) poly[VEIM]Br under nitrogen flow.

2.3. Preparation of PEI/CNT films

Various loading amounts (0.1–3.0 wt.%) of CNTs (pristine, oxidized or PIL functionalized) were ultrasonicated in PEI solutions in dichloromethane (DCM) (0.23 g/mL) for 30 min. The resulted dispersions were casted into Teflon-coated aluminum foil molds and the solvent was allowed to evaporate slowly at room temperature. All the composite films were further dried in a vacuum oven first at 100 °C for 2 days, then at 150 °C for 1 day to remove completely the residual solvent. Then, the obtained composites were compression molded under a pressure of 240 bars at 250 °C for 4 min.

2.4. Characterization techniques

The IR spectra were recorded on a 1710 Fourier Transform spectrophotometer using KBr salt for solid pellet analysis. ATR-FTIR measurements were performed using a PerkinElmer Spectrum 100 Universal ATR-FTIR. The particle size analysis of CNT dispersions was performed with a Mastersizer 2000. ^{1}H NMR (300 MHz) spectra were recorded on a Bruker DPX-300 spectrometer. The carbon nanotube solutions for casting were sonicated using an ultrasonic probe (Vibra Cell 75115, 500 W, Bioblock Scientific) at amplitude of 20% in an ice bath. Thermogravimetric analysis was performed using a TA Instruments Q50 (10 °C min^{-1} under 60 mL min^{-1} N_2). Differential scanning calorimetry (DSC) measurements were conducted using a TA Instruments Q200 differential scanning calorimeter in a nitrogen atmosphere (10 °C min^{-1}, flow rate = 50 mL min^{-1}). To erase the thermal history of the samples, each sample was scanned two times between −60 °C and 300 °C. The stress–strain curves of the composites were obtained using an Instron model 5565 mechanical tester at 20–21 °C. The strain speed was 5 mm min^{-1} under a load of 1 kN. The values reported here represent an average of the results for tests run on at least five specimens. Dynamic mechanical analysis (DMA) was conducted on the Mettler Toledo DMA/SDTA861e in tension mode. DMA analysis was conducted on $5.5 \times 4 \times 0.5$ mm^3 samples. The heating rate was 3 °C/min within a 25–240 °C range and the frequency 1 Hz. Maximum limits of stress (5 N) and strain (12 μm) were used to assure linear viscoelastic behavior. A JEOL JSM 6700F Field Emission Gun (FEG) scanning electron microscope was used to obtain SEM images. The microtomed slices (70 nm) of composites were placed on copper grids and examined by TEM

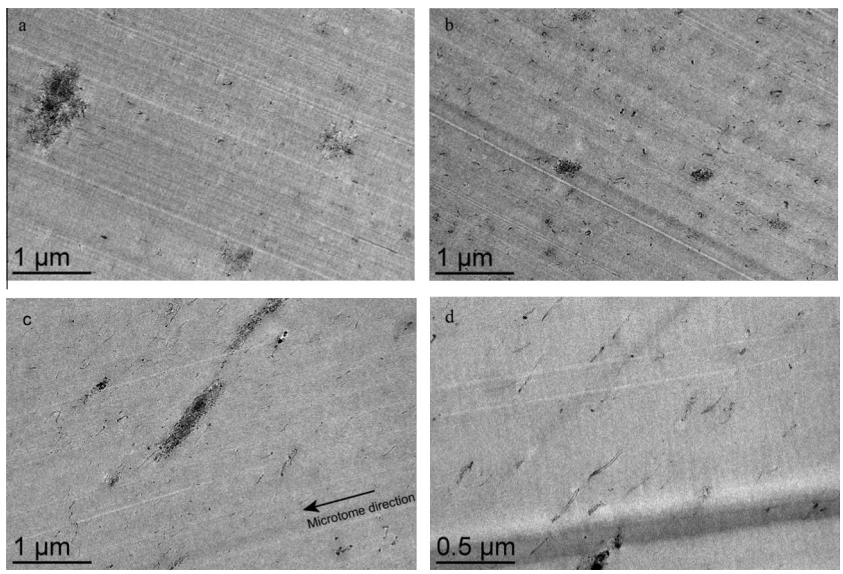

Fig. 4. TEM micrographs of PEI/CNT composite films at 1 wt.% loading of (a) pristine CNT, (b) oxidized CNT and (c) and (d) CNT–PIL.

Table 1
Tensile properties of neat PEI and PEI/CNT composites.

Sample	CNT loading (wt.%)	Young's modulus (GPa)	Yield stress (MPa)	Yield strain (%)	Stress at break (MPa)	Strain at break (%)
Neat PEI	0	2.69 ± 0.05	95.0 ± 2.7	6.2 ± 0.5	79.5 ± 2.8	10.0 ± 3.9
PEI/pristine CNTs	0.1	2.69 ± 0.12	94.6 ± 3.1	6.1 ± 0.4	79.5 ± 3.8	13.6 ± 5.0
	0.3	2.69 ± 0.02	93.2 ± 1.2	6.1 ± 0.3	79.1 ± 3.0	12.9 ± 6.3
	0.6	2.62 ± 0.12	93.9 ± 1.7	6.4 ± 0.3	79.5 ± 5.9	13.7 ± 7.4
	1	2.71 ± 0.05	92.1 ± 1.4	6.1 ± 0.2	77.9 ± 3.5	9.7 ± 2.2
	3	2.76 ± 0.05	92.5 ± 6.2	5.5 ± 0.9	84.2 ± 5.4	6.2 ± 1.7
PEI/oxidized CNTs	0.1	2.63 ± 0.04	93.4 ± 2.4	6.1 ± 0.5	86.8 ± 6.0	8.4 ± 4.6
	0.3	2.67 ± 0.08	92.3 ± 1.2	5.9 ± 0.3	79.1 ± 2.4	10.3 ± 5.0
	0.6	2.64 ± 0.05	93.2 ± 1.7	6.3 ± 0.1	77.1 ± 1.0	15.7 ± 6.7
	1	2.64 ± 0.08	92.3 ± 2.5	6.0 ± 0.4	79.7 ± 7.3	7.8 ± 1.9
PEI/CNT–PIL	0.1	2.65 ± 0.06	92.5 ± 1.9	6.1 ± 0.1	78.7 ± 2.5	14.4 ± 6.3
	0.3	2.75 ± 0.08	96.1 ± 3.3	6.2 ± 0.1	83.5 ± 9.5	7.8 ± 1.6
	0.6	2.62 ± 0.09	94.7 ± 3.2	6.2 ± 0.4	82.9 ± 6.1	11.6 ± 5.0
	1	2.56 ± 0.04	90.0 ± 2.9	5.5 ± 0.7	84.8 ± 7.0	6.1 ± 1.4

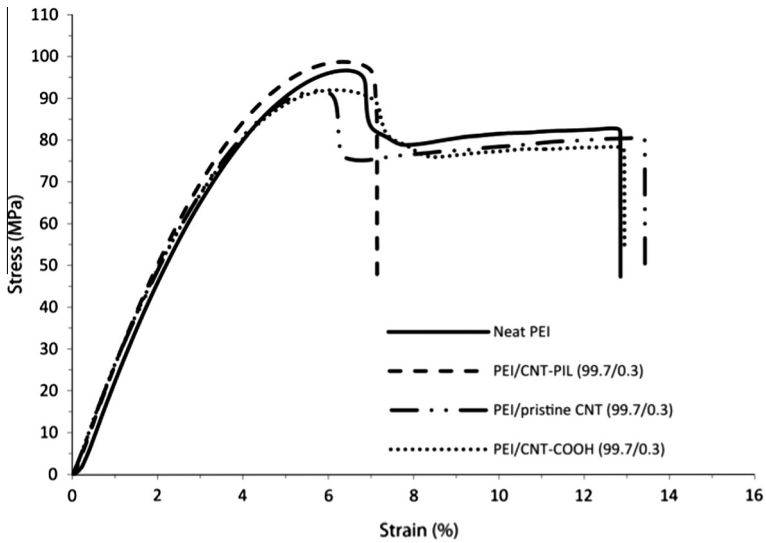

Fig. 5. Typical tensile stress–strain curves of neat PEI and PEI/CNT composites.

using a JEOL JEM-1400 at 120 kV. An Agilent 4156C precision semiconductor parameter analyzer equipped with a 16442A test fixture was used to measure the electrical resistivity of the samples. The 0.5 mm thick CNT/PEI composite films were cut into rectangular specimens of 20 mm × 10 mm, and upper and lower surfaces of the specimens were coated with conducting silver paint to ensure an intimate contact between the specimen surfaces and electrodes.

3. Results and discussion

3.1. Functionalization of CNTs with PIL

PEI is soluble in halogenated solvents such as chloroform, dichloromethane (DCM), and in *N*-methyl-2-pyrrolidone (NMP). To disperse PIL functionalized CNTs in DCM, the DBS ($C_{12}H_{25}C_6H_4SO_3^-$) anion was chosen as the PIL counter-anion. Pristine CNTs were functionalized by poly[VEIM]Br following the *in situ* polymerization method [14] followed by anion-exchange. Indeed, preliminary experiments performed in our laboratory has shown that this procedure is more efficient to get high PIL loading than the direct *in situ* polymerization of poly[VEIM]DBS. This is presumably due to the steric effect of the anion. The TEM image in Fig. 2 shows the presence of a continuous thin polymer layer (1.7 nm thickness) around the CNTs. The TGA profiles of the resulting functionalized CNTs show the decomposition steps of the PIL component under inert atmosphere (Fig. 3). All the samples decomposed in two major steps. It is observed that adsorbed PILs start to degrade at a lower temperature compared to neat PILs (Table S1 in SD), which may be due to: i) changes in the PIL structure as a result of the interaction with CNTs [15], the presence of traces of iron catalyst on pristine CNT surface, which may react with the sulfonate counter-ion and hence catalyze the PIL decomposition process. TGA analysis shows that CNT–poly[VEIM]DBS contains 19 wt.% PIL.

According to the TGA data, approximately 80% of the Br anions could be exchanged with DBS. As expected, the FTIR spectra of the PIL functionalized CNTs display the absorbance bands of the corresponding PILs (Fig. S2 in SD). Thus, the IR spectra of both PIL functionalized CNT samples show the bands attributed to the poly[VEIM]$^+$ cation in the 2800–3200 cm^{-1} region and at 1550 cm^{-1}. Moreover, in the spectrum of CNT–poly[VEIM]DBS, the characteristic bands of the $C_{12}H_{25}C_6H_4SO_3^-$ anion [16], S=O asymmetrical stretching band at 1193 cm^{-1}, CH aromatic bending bands at 833 cm^{-1}, 1010 cm^{-1} and 1026 cm^{-1} are clearly observed.

After 30 min sonication in DCM, a black suspension was observed for all three types of CNTs (pristine, oxidized and PIL functionalized). However, it was possible to observe with the naked eye that the dispersions of pristine and oxidized CNTs contained large agglomerates, while the PIL functionalized CNTs dispersed better. To evaluate the quality of the CNT dispersions, particle size analysis by laser diffraction technique was carried out. The diameter of the sphere of the equivalent volume corresponding to an individual nanotube should be between 0.025 and 0.15 μm. The measurements confirmed that the dispersions of both pristine and oxidized CNTs in DCM were unstable. The volume weighted mean diameter (D[4,3]) values of three measurements ranged from 27.9 to 53.2 μm and from 13.3 to 34.8 μm for pristine and oxidized CNTs, respectively. On the contrary, CNT–PIL gave very stable dispersions in DCM with a D[4,3] of 13.0 μm (±0.2), and as seen from the particle size distribution graphs the number of small particles (below 0.5 μm) was higher in this sample (Fig. S3 in SD).

3.2. Incorporation of CNTs into the polymer matrix

A series of PEI/CNT films was prepared from PEI and the three types of CNTs. The ATR-FTIR spectra of the composites (at 0.1 wt.% CNT loading) were the same as the spectrum of neat PEI (Fig. S4 in SD). We observed the characteristic carbonyl bands of imide at 1777 cm^{-1} and 1716 cm^{-1} and C–N stretching band at 1350 cm^{-1}. The TEM micrographs in Fig. 4 show the CNT distribution in the polymer matrix at 1 wt.% CNT loading. While all samples contain agglomerated CNTs, a more pronounced debundling was noticed for the samples containing modified CNTs, with a relatively large proportion of individual CNTs. Moreover, TEM analysis reveals an interesting feature on the morphology of the PEI/CNT–PIL composite. In Fig. 4c, it is observed that CNTs present a preferential alignement. Macroscopic self-organizing alignment [17], or self-assembly [18] of CNTs in a polymer-nanocomposite, probably arising from solvent–polymer interactions, has been already reported.

3.3. Mechanical, thermal and electrical properties of the composites

The results in terms of Young's modulus, yield stress and strain of the films are reported in Table 1. Fig. 5 shows typical tensile stress–strain curves obtained for the films. By introduction of CNTs, no major reinforcement was obtained in terms of tensile modulus and yield. It is worth noting that PEI and PIL do not form any miscible polymer blend. When loaded in excess of 1 wt.% CNT, the films became very brittle (see Fig. 6). The brittleness of the

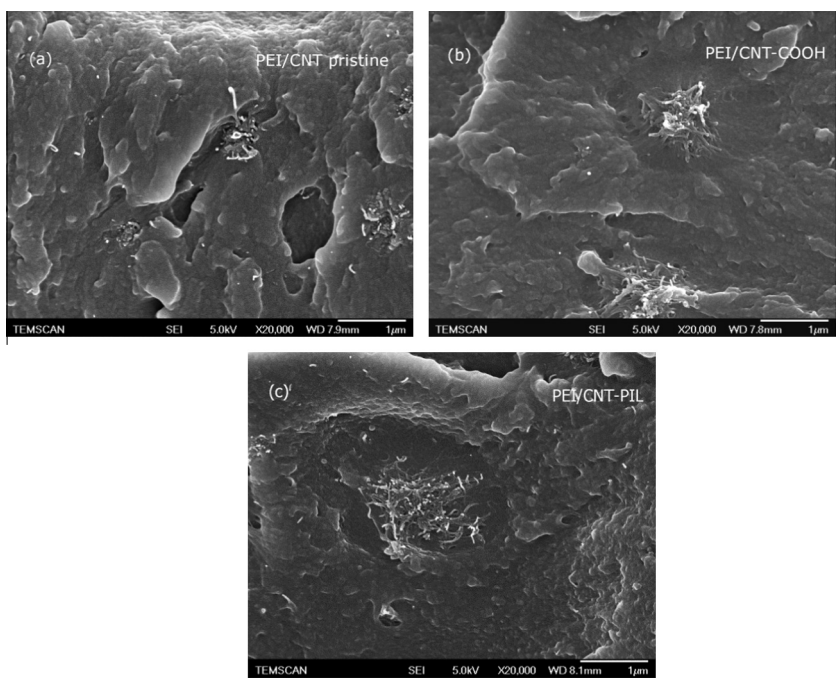

Fig. 6. SEM micrographs of the failure surfaces of PEI/CNTs composites at 1 wt.% CNT loading.

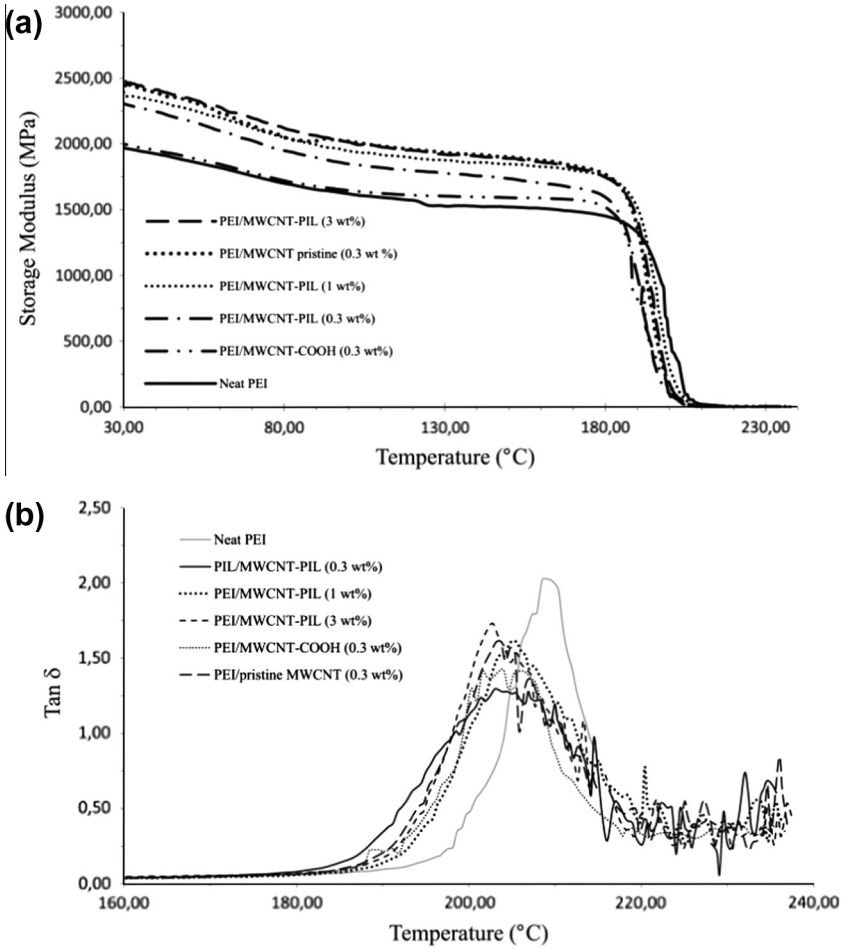

Fig. 7. DMA curves of (a) storage modulus and (b) tanδ versus temperature for PEI and PEI/CNT composites.

Table 2
Thermal properties of PEI and PEI/CNT composites.

Sample	CNT loading (wt.%)	T_g (by DSC) (°C)	T_d (by TGA) (°C) (at 5 wt.% loss)
Neat PEI	0	213	494
PEI/pristine CNTs	0.1	214	505
	0.3	210	503
	0.6	212	504
	1	206	505
	3	211	505
PEI/oxidized CNTs	0.1	212	504
	0.3	206	504
	0.6	213	502
	1	213	502
	3	207	502
PEI/CNT–PIL	0.1	210	500
	0.2	214	504
	0.3	209	503
	0.4	211	505
	0.6	215	502
	1	213	499
	3	211	502

composites at a loading of 3 wt.% oxidized CNTs and CNT–PIL did not allow any sampling.

SEM micrographs of the tensile fractured surfaces of all three composite films show agglomerates of CNTs being pulled half way out from the matrix and revealing a surface pattern characteristic of brittle fracture. In addition, it is clear that alignment of the CNTs is not produced by cutting the sample (because direction of CNT alignment and microtome are not the same). It could be probably induced during preparation of the sample. Moreover, when PIL modified MWCNTs are used, the dispersion of the CNTs is better observed and, in consequence, the alignment direction is clearly observed for non-agglomerated CNTs. Fig. 7 displays the dynamic mechanical spectra as a function of temperature for PEI and PEI/CNT composites. The storage modulus (E') of the PEI/CNT composites containing CNT–PIL is higher than that of neat PEI in the temperature range 30–190 °C. There is no significant difference in storage modulus between different loadings (0.3 and 3 wt.%). At a loading of 3 wt.%, an improvement of around 25% in storage modulus was obtained. However, a similar increase was also obtained in the case of pristine CNTs. The damping ($\tan\delta$) peaks of all the PEI/CNT composites showed a decrease in maximum peak height, from 2.02 for pure PEI to 1.29 for PEI/CNT–PIL composite at 0.3 wt.% loading. The height of the damping peaks reveals the efficiency of the stress transfer to the CNTs, which depends on the CNT/matrix adhesion [5,19]. This is, dissipation of PEI/CNT composite systems is broader than dissipation of pure PEI, showing the maximum of the peak for nanocomposites a decrease of 5 °C in regard to pure PEI. This behavior could be attributable to a different relaxation spectrum for PEI chains in function of the degree of dispersion of the MWCNTs. The decrease of the T_g position in presence of carbon nanotubes is quite unexpected from the point of view of classical fiber-reinforcement mechanics and suggests an increase in free volume in nanocomposites in regard to the neat polymer. In consequence, dispersion and interfacial stress transfer is the highest for PEI/MWCNT–PIL composite at 0.3 wt.% loading. As observed from the $\tan\delta$ versus temperature graphs in Fig. 7b, the T_g of the neat PEI appeared at approximately 209 °C while the T_g of the PEI/CNT composites shifted to a lower temperature by around 5 °C.

In order to investigate the thermal behavior of the neat PEI films and the PEI/CNTs films, TGA and DSC analyses were carried out. All PEI/CNT composites show an overall higher thermal stability compared to the neat PEI (Table 2). Incorporation of CNTs increased the degradation temperature of the composites by up to 11 °C.

The room temperature volume resistivity of the neat PEI was measured to be 3.1×10^{12} Ω cm. The introduction of 3 wt.% of pristine CNTs dramatically decreased the volume resistivity of the composite film to 1.3×10^{3} Ω cm, indicating that the percolation threshold lies between 1 and 3 wt.% of pristine CNTs. However, no improvement in conductivity was observed for composites loaded with oxidized or PIL functionalized CNTs at concentrations up to 3 wt.%. As non-covalent PIL modification process does not disrupt the π-conjugation system of the nanotubes, the low conductivity could be attributed to the insulating PIL layer around the CNTs, which could inhibit the efficient charge transfer between CNTs as already reported for several polymer wrapped CNTs [20]. Yet, there are examples where electrical conductivity has been achieved with similar PIL coated CNTs [4,21]. Another possible explanation could arise from the alignment of CNTs. Indeed, it has been shown that the lowest percolation threshold and the maximum conductivity occur when CNTs are randomly oriented and reaggregated in the matrix [22,23].

4. Conclusions

Three MWCNT materials were mixed with PEI by a solution-based processing method to prepare thin films of composites. Prior to composite processing the MWCNT materials were characterized by TGA, IR and TEM. The first nanotube material consists in pristine CNTs that showed a loosely packed agglomerate morphology. The second MWCNT sample consists in HNO_3 oxidized pristine CNT, and contains a significant concentration of covalently grafted surface acidic group. The third MWCNT sample consists in pristine CNTs non-covalently functionalized with polymerized ionic liquid thin films of approximately 2 nm. This latter sample shows a better dispersion in dichloromethane. Additionally, in the PEI composite thin films prepared from CNT–PIL, a preferential orientation of CNT bundles and individual CNTs has been observed.

The incorporation of CNTs does not have much influence on the tensile properties the composites. The incorporation of CNTs led to a moderate increase of up to 25% (CNT–PIL, 3 wt.%) in storage modulus of the PEI composites. The lowered height of the damping ($\tan\delta$ peaks shows that there is indeed stress transfer to CNTs and it is most efficient at 0.3 wt.% CNT–PIL loading. The electrical resistivity of the composite decreased by nine orders of magnitude at 3 wt.% loading of pristine CNTs, whereas for the same loading of modified CNTs no improvement was noticed. These results can be rationalized as follow. In the case of oxidized CNT, damages of CNT structure can explain the low electrical conductivity. For CNT–PIL, the presence of an electrically insulating thin film on the CNT surface and the fact that CNT–PIL are partially aligned in the composite could explain the low electrical conductivity. According to DMA analysis, addition of CNTs reduces T_g by about 5 °C. Furthermore, the thermal stability of the polymer composite increased by *ca* 10 °C whatever the type of CNT used.

Further studies are on-going to evaluate the importance of the processing methods on the final properties of the composites.

Acknowledgements

The authors acknowledge the financial support from the European Project POCO, 7th Framework Programme, Contract No. CP-IP 2139391. We also thank Aitor Larrañaga Espartero for his assistance with DMA and Nicolas Mauran for the electrical measurements.

Appendix A. Supplementary material

Supplementary data associated with this article can be found, in the online version, at http://dx.doi.org/10.1016/j.eurpolymj.2013.08.007.

References

[1] Rahmat M, Hubert P. Carbon nanotube–polymer interactions in nanocomposites: a review. Compos Sci Technol 2011;72(1):72–84.
[2] Sahoo NG, Rana S, Cho JW, Li L, Chan SH. Polymer nanocomposites based on functionalized carbon nanotubes. Prog Polym Sci 2010;35(7):837–67.
[3] Tunckol M, Durand J, Serp P. Carbon nanomaterial–ionic liquid hybrids. Carbon 2012;50(12):4303–34.
[4] Tung TT, Kim TY, Suh KS. Nanocomposites of single-walled carbon nanotubes and poly(3,4-ethylenedioxythiophene) for transparent and conductive film. Org Electron 2011;12(1):22–8.
[5] Kumar S, Sun LL, Lively B, Zhong WH. Thermal and Mechanical enhancements of polyetherimide/multi-walled carbon nanotube composite performance using "Solid Nano-Nectar" assisted melt dispersion. J Nanosci Nanotechnol 2011;11(3):1976–85.
[6] Kumar S, Li B, Caceres S, Maguire RG, Zhong W-H. Dramatic property enhancement in polyetherimide using low-cost commercially functionalized multi-walled carbon nanotubes via a facile solution processing method. Nanotechnology 2009;20(46):465708.
[7] Goh PS, Ng BC, Ismail AF, Aziz M, Sanip SM. Surfactant dispersed multi-walled carbon nanotube/polyetherimide nanocomposite membrane. Solid State Sci 2010;12(12):2155–62.
[8] Shao L, Bai Y-P, Huang X, Meng L-H, Ma J. Fabrication and characterization of solution cast MWNTs/PEI nanocomposites. J Appl Polym Sci 2009;113(3):1879–86.
[9] Solhy A, Machado BF, Beausoleil J, Kihn Y, Gonçalves F, Pereira MFR, et al. MWCNT activation and its influence on the catalytic performance of Pt/MWCNT catalysts for selective hydrogenation. Carbon 2008;46(9):1194–207.
[10] Gerber I, Oubenali M, Bacsa R, Durand J, Goncalves A, Pereira MF, et al. Theoretical and experimental studies on the carbon-nanotube surface oxidation by nitric acid: interplay between functionalization and vacancy enlargement. Chemistry 2011;17(41):11467–77.
[11] Eitan A, Jiang K, Dukes D, Andrews R, Schadler LS. Surface modification of multiwalled carbon nanotubes: toward the tailoring of the interface in polymer composites. Chem Mater 2003;15(16):3198–201.
[12] Marcilla R, Alberto Blazquez J, Rodriguez J, Pomposo JA, Mecerreyes D. Tuning the solubility of polymerized ionic liquids by simple anion-exchange reactions. J Polym Sci Part A: Polym Chem 2004;42(1):208–12.
[13] Marcilla R, Blazquez JA, Fernandez R, Grande H, Pomposo JA, Mecerreyes D. Synthesis of novel polycations using the chemistry of ionic liquids. Macromol Chem Phys 2005;206(2):299–304.
[14] Tunckol M, Fantini S, Malbosc F, Durand J, Serp P. Effect of the synthetic strategy on the non-covalent functionalization of multi-walled carbon nanotubes with polymerized ionic liquids. Carbon 2013;57:209–16.
[15] Hong S, Tung T, Huyen Trang L, Kim T, Suh K. Preparation of single-walled carbon nanotube (SWNT) gel composites using poly(ionic liquids). Colloid Polym Sci 2010;288(9):1013–8.
[16] Xu ZP, Braterman PS. High affinity of dodecylbenzene sulfonate for layered double hydroxide and resulting morphological changes. J Mater Chem 2003;13(2).
[17] Chen W, Tao X. Self-organizing alignment of carbon nanotubes in thermoplastic polyurethane. Macromol Rapid Commun 2005;26(22):1763–7.
[18] García-Gutiérrez MC, Nogales A, Rueda DR, Domingo C, García-Ramos JV, Broza G, et al. Templating of crystallization and shear-induced self-assembly of single-wall carbon nanotubes in a polymer-nanocomposite. Polymer 2006;47(1):341–5.
[19] Sarasua JR, Pouyet J. Dynamic mechanical behavior and interphase adhesion of thermoplastic (PEEK, PES) short fiber composites. J Thermoplast Compos Mater 1998;11(1):2–21.
[20] Zeng Y, Liu P, Du J, Zhao L, Ajayan PM, Cheng H-M. Increasing the electrical conductivity of carbon nanotube/polymer composites by using weak nanotube–polymer interactions. Carbon 2010;48(12):3551–8.
[21] Fukushima T, Kosaka A, Yamamoto Y, Aimiya T, Notazawa S, Takigawa T, et al. Dramatic effect of dispersed carbon nanotubes on the mechanical and electroconductive properties of polymers derived from ionic liquids. Small 2006;2(4):554–60.
[22] Du F, Fischer JE, Winey KI. Effect of nanotube alignment on percolation conductivity in carbon nanotube/polymer composites. Phys Rev B 2005;72(12):121404.
[23] Bryning MB, Islam MF, Kikkawa JM, Yodh AG. Very low conductivity threshold in bulk isotropic single-walled carbon nanotube–epoxy composites. Adv Mater 2005;17(9):1186–91.